Solid State Science and Technology, Vol. 20, No 1 & 2 (2012) 88-95
ISSN 0128-7389

SELF-CONSISTENT CALCULATION WITH ADAPTIVE BOUNDARY CONDITION OF ELECTRON STATES IN SILICON *n*-MOS NANOSTRUCTURES

G. Gopir [1], Y. Y. Khoo[1], C. Y. Woon[1] and A. P. Othman[2]

[1]*School of Applied Physics, Faculty of Science and Technology, Universiti Kebangsaan Malaysia, 43600 Bangi, Selangor Malaysia*

[2]*Institute of Space Science (ANGKASA), Universiti Kebangsaan Malaysia, 43600 Bangi, Selangor, Malaysia*

Corresponding author: gerigopir@gmail.com

ABSTRACT

We develop a computational procedure to calculate the properties of electron states in a Si *n*-MOS inversion layer by discretizing and iteratively solving the differential Schrödinger and Poisson equations using centered finite differences. In this self-consistent calculation, we apply an adaptive boundary condition to the wave function and confining potential at the bulk side of the nanostructure; and incorporate Fermi-Dirac distribution for the ionized acceptor density in the inversion and depletion layers. This requires relatively simpler inputs and we are able to determine the various parameters of the electron state subbands. We compared our results with those published in the literature applying self-consistent Schrödinger-Poisson calculation on similar Si *n*-MOS nanostructures.

Keywords: MOS inversion layer; nanostructure; self-consistent calculation; Schrödinger-Poisson; electron state

INTRODUCTION

The self-consistent method based on iterative solutions of the Schrödinger and Poisson equations was developed in the 1970s to calculate the properties of electron states in an *n*-channel metal oxide semiconductor (*n*-MOS) nanostructure which consists of a metal gate, an oxide layer of silicon dioxide (SiO_2) and a *p*-doped semiconductor layer of silicon [1]. Since then the self-consistent method has been expanded and applied to model and simulate the electronic and optical properties of other semiconductor nanostructures and devices such as quantum well, quantum wire, quantum dot, photodetector and transistor [2-9]. Self-consistent calculations produce various material parameters by incorporating factors such as Hartree potential, gate potential, electric field, doping, exchange-correlation, strain and piezoelectric field. However, these calculations usually use variational method to derive the trial potential profile and relaxation of potential to achieve self-consistency, requiring more complicated input parameters. We hereby apply a combination of adaptive boundary condition for the

Solid State Science and Technology, Vol. 20, No 1 & 2 (2012) 88-95
ISSN 0128-7389

wave function and confining potential; and Fermi-Dirac distribution for the ionized acceptor density to achieve faster convergence and self-consistency in the Schrödinger-Poisson calculation of this nanostructure system.

THEORY

Using the effective mass approximation, the one-dimensional Schrödinger equation of electron states in the MOS nanostructure is

$$-\frac{\hbar^2}{2m}\frac{d^2\psi}{dz^2} - e\phi(z)\psi(z) = E\psi(z) \quad . \tag{1}$$

where m is the electron effective mass, e is the electron charge; and the potential energy of the Hamiltonian, $V(z)$, is assumed to contain only the Hartree component, $V(z) = -e\phi(z)$. The Schrödinger equation is solved to obtain the subband energy (eigenvalue), E_i, and wave function (eigenfunction), ψ_i, of the quantized electron states. Then the energies and wave functions of the occupied subbands of i are used in the Poisson equation,

$$\frac{d^2\phi}{dz^2} = -\frac{1}{\varepsilon_r\varepsilon_0}\left[\rho_d(z) - e\sum_i N_i|\psi_i(z)|^2\right] \tag{2}$$

to calculate the Hartree or electrostatic potential $\phi(z)$. Here ε_0 is the dielectric constant of free space, $\varepsilon_r = 11.7$ is the relative permittivity of the Si [1,9] semiconductor layer and N_i is the sheet density of subband i at absolute temperature T given by

$$N_i = \frac{n_v m k_B T}{\pi\hbar^2} ln\left[1 + \exp\left(\frac{E_F - E_i}{k_B T}\right)\right] \tag{3}$$

with k_B the Boltzmann constant, $\hbar$ the reduced Planck constant, E_F the Fermi energy and n_v the degeneracy of the conduction band valley. For Si, m at the conduction band valley is either along the longitudinal direction with value 0.916 m_e and $n_v = 2$; or along the transverse direction with value 0.190 m_e and $n_v = 4$. The depletion region charge density of $\rho_d(z)$ is related to the three-dimensional ionized donor and acceptor densities of $N_D^+(z)$ and $N_A^-(z)$, respectively, by $\rho_d(z) = e[N_D^+(z) - N_A^-(z)]$. Two models are used to determine the ionized doping densities. The first model, simpler and valid at high temperatures, assumes that the dopant atoms are fully ionized ($f_A = 0$) and requires the value of the depletion layer thickness z_d [2,4,9],

$$N_{D,A}^{\pm} = \begin{cases} N_{D,A} & z \le z_d \\ 0 & z > z_d \end{cases} \quad . \tag{4}$$

The second model of ionized doping densities assumes that the densities of the ionized dopants follow a Fermi-Dirac distribution ($f_A = 1$) [6,8],

$$\begin{aligned} N_D^+(z) &= \frac{N_D}{1 + 2exp\left[\frac{E_F - e\phi(z) - E_D}{k_B T}\right]} \\ N_A^-(z) &= \frac{N_A}{1 + g_v exp\left[\frac{E_A - e\phi(z) - E_F}{k_B T}\right]} \end{aligned} \tag{5}$$

where E_A and E_D are the respective activation energies of the acceptors and donors in the doped semiconductor material; and g_v is the degeneracy of the valence band valley. Thus, in this model the ionized doping densities are functions of temperature, activation energy, Fermi energy, local potential and band valley degeneracy. For Si, E_A and E_D are around 50 meV [3]; and $g_v = 4$ [8]. In this study, we assume that the semiconductor layer is *p*-doped, $N_D = 0$, leading to an *n*-channel MOS nanostructure. The Fermi energy level is determined from charge conservation by $N_s = \sum_{i=1}^{M} N_i$, where the inversion layer sheet density N_S is equal to the total sheet densities of the M lowest occupied electron subbands. Thus, the subband occupation factor of subband i is $f_i = N_i/N_S$. At absolute zero, $T = 0$ K, N_i reduces to $N_i(T=0) = \frac{n_v m}{\pi \hbar^2}(E_F - E_i)\Theta(E_F - E_i)$; and for *p*-doping $N_A^-(z, T=0) = N_A \Theta\left(E_A - E_F - e\phi(z)\right)$ [8] with $\Theta(x)$ the Heaviside step function, $\Theta(x) = \begin{cases} 1 & x > 0 \\ 0 & x \leq 0 \end{cases}$.

The average lenth of subband i from the oxide interface is

$$z_i = \frac{\int z|\psi_i(z)|^2 dz}{\int |\psi_i(z)|^2 dz} = \frac{\sum_j z_j |\psi_i(z_j)|^2}{\sum_j |\psi_i(z_j)|^2} = \sum_j z_j |\psi_i(z_j)|^2 \quad (6)$$

where the subband wave functions are orthonormal, $\int \psi_i^*(z)\psi_j(z)\,dz = \delta_{ij}$. The average length of electrons in the inversion or depletion layer is then

$$z_{av} = \frac{\sum_i z_i N_i}{\sum_i N_i} = \frac{\sum_i z_i N_i}{N_s} \quad (7)$$

The sheet density of the depletion layer for uniform step size, $\Delta z_j = \Delta z$, is

$$N_d = \int N_A^-(z)dz = \sum_j N_A^-(z_j)\Delta z_j = \Delta z \sum_j N_A^-(z_j) \quad (8)$$

In this self-consistent calculation, the second order Schrodinger and Poisson differential equations are numerically solved consecutively and iteratively using second order finite differences, $\frac{d^2 f_j}{dz^2} \approx \frac{f_{j-1} - 2f_j + f_{j+1}}{\Delta z^2}$. We assume that the wave functions vanish at the oxide layer of infinite potential and at the depletion layer length, $\psi(0) = \psi(z_d) = 0$. The Hartree potential is defined as zero at the oxide interface, $\phi(0) = 0$, and constant at the bulk end, $\phi'(z_d) = 0$. Here z_d is defined as the distance where the confining potential becomes constant, $\phi(z_j) = \phi(z_{j-1}) \Rightarrow z_d = z_j$. Our z_d changes with iteration, and we define this as the adaptive boundary condition. The convergence of the potential and energy levels are usually used as the stopping criteria but here we just iterate until 100 steps and monitor the valus of these parameters.

RESULT AND DISCUSSION

Table 1 presents the results of the self-consistent Schrodinger-Poisson calculation for the two lowest electron states in the inversion layer of the Si *n*-MOS nanostructure at $T = 0$ K using $N_A = 1 \times 10^{15}$ cm^{-3}, $m = 0.916\, m_e$, $n_v = 2$ and various valus of N_s. Our calculation results, shown as (1), are for ionized acceptor densities at both $f_A = 0$ (all

Solid State Science and Technology, Vol. 20, No 1 & 2 (2012) 88-95
ISSN 0128-7389

dopants ionized) and f_A = 1 (ionized according to Fermi-Dirac distribution). There is no significant difference in the values of the calculated parameters between the ionized acceptor density models, except for the sheet density of the depletion layer, N_d. In (2) are the published results of [1] with similar input parameters but using the condition of f_A = 0. Compared to the results of [1], our calculated values of E_0 are similar, our z_0 are comparable and our N_d are ~10^3 smaller.

Table 1: Self-consistent Schrodinger-Poisson calculation results for electron states in the inversion layer of the Si n-MOS nanostructure T = 0 K. Shown in (1) are the results of the present calculation and in (2) are the published results of [1] for similar input parameters

	N_s (10^{12} cm^{-2})	1	2	5	10
(1)	V_d (meV)	45.5	93.5	198.9	331.7
	z_d (nm)	2.7	3.1	3.1	3.0
	E_F (meV)	75.2	107.2	197.1	306.8
	E_0 (meV)	73.9	104.6	190.6	303.3
	E_1 (meV)	184.2	191.6	280.6	406.1
	z_0 (nm)	1.56	1.60	1.36	1.14
	z_0' (nm)	2.95	3.03	2.58	2.15
	z_1 (nm)	1.68	1.93	2.02	2.02
	f_0 (%)	100.0	100.0	100.0	100.0
	f_1 (%)	0.0	0.0	0.0	0.0
	N_d (10^8 cm^{-2}) (f_A=0)	2.7	3.1	3.1	3.0
	N_d (10^8 cm^{-2}) (f_A=1)	0.8	1.0	1.1	1.1
(2)	E_0 (meV)	71.5	108.7	195.1	306.8
	z_0 (nm)	4.26	3.56	2.72	2.19
	N_d (10^{11} cm^{-2})	1.207	1.204	1.198	1.192

Our simulation results at room temperature, T = 300 K, with material parameters similar to [9] and f_A = 0 are shown in Table 2 for the calculated E_i, P_i, z_i and their respective standard errors for subband i of the M = 5 lowest electron states. Here, we used $N_A = 5 \times 10^{17}$ cm^{-3} and $N_s = 1 \times 10^{13}$ cm^{-2}. The results of the present calculation are shown in (1) and the published results of [9] are shown in (2). Table 3 presents the respective results for f_A = 1 and Table 4 presents some of the derived paremeters.

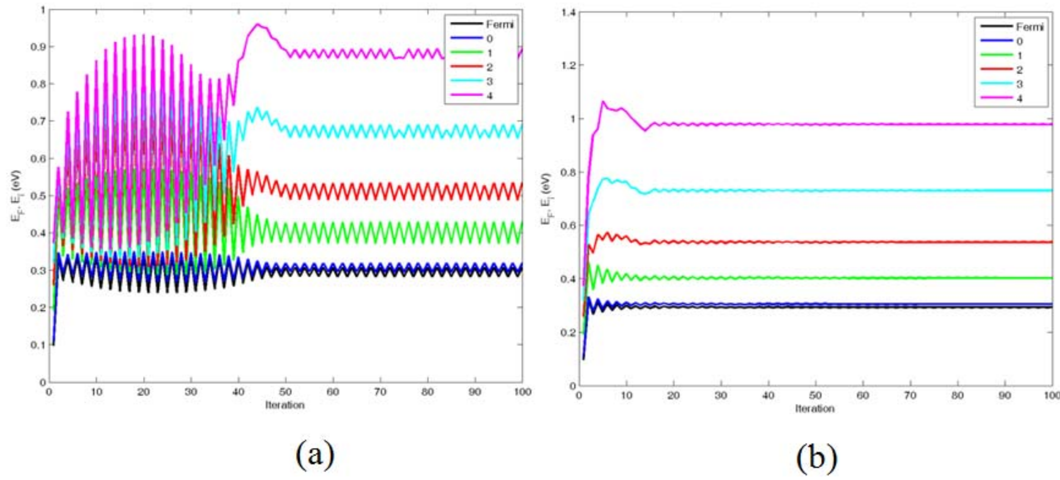

Figure 1: Variation with iteration of calculated E_F and E_i of the 5 lowest electron states in a Si n-MOS inversion layer at 300K for (a) f_A = 0 and for (b) f_A = 1

Table 2: Self-consistent Schrodinger-Poisson calculation results for 5 lowest electron states in the inversion layer of the Si *n*-MOS nanostructure at T = 300 K and f_A = 0. The results of the present calculation with f_A = 0 are shown in (1) and the published results of [9] are shown in (2)

		(1)						(2)		
m, n_v	i	E_i (meV)	ΔE_i (meV)	f_i (%)	Δf_i (%)	z_i (nm)	Δz_i (nm)	E_i (eV)	P_i (%)	z_i (nm)
$m_l = 0.916\ m_e$	0	307.0	6.8	96.3	1.3	1.15	0.14	245.3	79.9	1.11
$n_v = 2$	1	400.7	17.1	4.0	1.3	2.32	0.02	355.4	3.4	2.39
	2	511.1	13.5	0.1	0.0	2.23	0.07	424.5	0.2	3.44
	3	672.5	10.6	0.0	0.0	2.17	0.05	-	-	-
	4	880.9	7.5	0.0	0.0	2.14	0.05	-	-	-
$m_t = 0.190\ m_e$	0	517.9	0.0	100.3	0.0	1.86	0.00	352.5	16.4(?)	2.28
$n_v = 4$	1	728.7	0.0	0.1	0.0	2.99	0.00	488.3	0.1	4.46
	2	1057.2	0.0	0.0	0.0	2.83	0.00	590.2	0.0	6.19
	3	1524.4	0.0	0.0	0.0	2.78	0.00	676.7	0.0	7.75
	4	2125.5	0.0	0.0	0.0	2.75	0.00	-	-	-

Solid State Science and Technology, Vol. 20, No 1 & 2 (2012) 88-95
ISSN 0128-7389

Table 3: Self-consistent Schrodinger-Poisson calculation results for 5 lowest electron states in the inversion layer of the Si *n*-MOS nanostructure at $T = 300$ K and with $f_A = 1$ anf $E_A = 50$ MeV

m, n_v	i	E_i (meV)	ΔE_i (meV)	f_i (%)	Δf_i (%)	z_i (nm)	Δz_i (nm)
$m_l = 0.916$	0	304.9	0.1	97.5	0.0	1.13	0.00
$n_v = 2$	1	402.7	0.1	2.9	0.0	2.15	0.00
	2	536.9	0.1	0.0	0.0	2.02	0.00
	3	729.9	0.1	0.0	0.0	1.97	0.00
	4	978.1	0.1	0.0	0.0	1.95	0.00
$m_t = 0.190$	0	513.8	0.0	100.3	0.0	1.82	0.00
$n_v = 4$	1	760.9	0.0	0.0	0.0	2.67	0.00
	2	1162.7	0.0	0.0	0.0	2.55	0.00
	3	1730.7	0.0	0.0	0.0	2.51	0.00
	4	2459.8	0.0	0.0	0.0	2.49	0.00

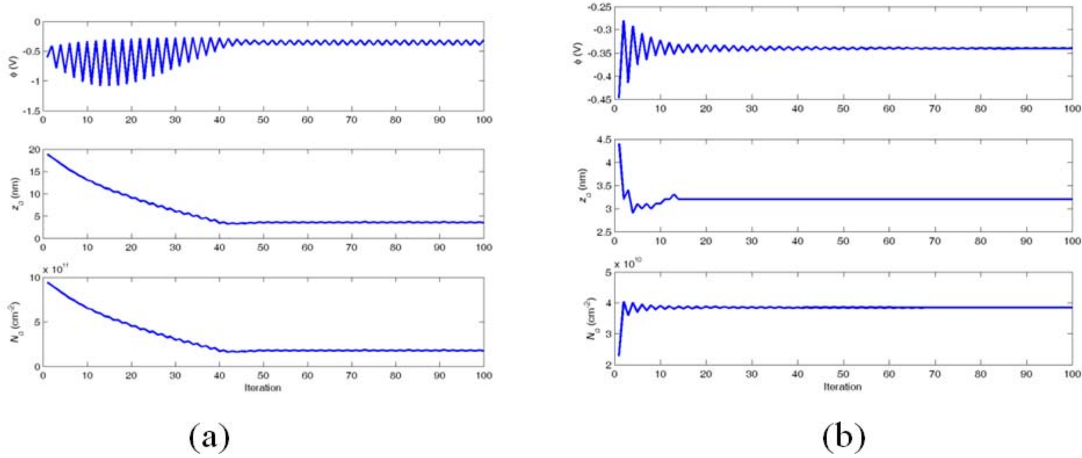

Figure 2: Variation of ϕ, z_d and $N_A^-(z)$ with iteration in the Si n-MOS inversion and depletion layer at 300 K for (a) $f_A = 0$ and for (b) $f_A = 1$

Figure 1 shows the variations of of E_F and E_i for the 5 lowest electron subbands for $f_A = 0$ and for $f_A = 1$ at 300 K. It is seen that $f_A = 0$ results in oscillations with energy uncertainties of around 10 meV and $f_A = 1$ leads to convergence at iteration steps of around 20. Figure 2 presents the corresponding variations of ϕ, z_d and $N_A^-(z)$ with iteration. A faster convergence is seen to be achieved with $f_A = 1$. From our calculations, we estimate z_{av} to be 1-2 nm and z_d ~3-4 nm.

Table 4: Summarised parameters for T = 300 K. Shown at the right side of each column are the errors of the calculated parameters

N_d^- option	0				1			
m	m_l		m_t		m_l		m_t	
E_F (meV)	294.9	7.3	540.4	0.0	293.3	0.0	536.3	0.0
V_d (meV)	354.8	23.6	556.5	0.0	340.5	0.2	534.5	0.0
z_d (nm)	3.6	0.1	4.8	0.0	3.2	0.0	4.3	0.0
N_d (10^{11} cm^{-2})	1.78	0.03	2.40	0.00	3.85	0.00	1.01	0.00
z_{av} (nm)	1.19	0.08	1.89	0.00	1.17	0.00	1.82	0.00

CONCLUSION

A self-consistent computational procedure using adaptive boundary condition has been developed to model electron states in a silicon *n*-MOS nanostructure. The use of adaptive boundary condition and Fermi-Dirac ionized donors results in faster convergence of output parameters and simpler input requirements. The obtained parameters could be further used to determine the optical properties of this nanostructure and other quantum devices.

\

ACKNOWLEDGMENT

We thank the Malaysian Ministry of Science, Technology and Innovation (MOSTI) for ScienceFund grant 03-01-02-SF0061 and Universiti Kebangsaan Malaysia for grant UKM-GUP-2011-354.

REFERENCES

[1] F. Stern, *Phys. Rev. B* **5** (1972) 4891-4899
[2] F. Stern & S. Das Sarma, *Phys. Rev. B* **30** (1984) 840-848
[3] S. M. Sze, Semiconductor Devics: Physics and Technology, Wiley, New York, 1985
[4] C. D. Simserides & G. P. Triberis, *J. Phys.: Condensed Matter* **5** (1993) 6437-6446.
[5] J. A. Cuesta, A. Sanchez & F. Dominguez-Adame, *Semicond. Sci. Technol.* **10** (1995) 1303-1309
[6] A. Trellakis & U. Ravioli, *Comput. Methods Appl. Mech. Engrg.* 181 (2000) 437-449
[7] E. Ozturk, Y. Ergun, H. Sari & I. Sokmen, *Semicond, Sci. Technol.* 16 (2001) 421-426

[8] V. V. Mitin, V. A. Kochelap & M. A. Stroscio, Quantum Heterostructures: Microelectronics and Optoelectronics, Cambridge University Press, Cambridge, UK, 1999

[9] C. Hamaguchi, Basic Semiconductor Physics, Springer, Berlin, 2001